DOI: 10.24874/ti.2063.11.25.01

Tribology in Industry

www.tribology.rs

RESEARCH

Optimizing SiC Content for Enhanced Corrosion Resistance in Al-5%Cu Alloys Fabricated by Powder Metallurgy

Lubna Ghalib[a,*], Sahib M. Mahdi[b], Esraa Ali Abbod[a]

[a]*Materials Engineering Department, Mustansiriyah University, Bab Al-Muadham 46049, Baghdad-Iraq,*
[b]*Engineering of Medical instrumentation Techniques Department, Ashur University, College of Engineering Technical, Baghdad-Iraq.*

Keywords:

Aluminum-copper alloy
Silicon carbide
Powder Metallurgy
Corrosion; Pitting
Electrochemical Properties

* Corresponding author:

Lubna Ghalib
E-mail:
lubnaghalib81@uomustansiriyah.edu.iq

Received: 11 November 2025
Revised: 26 December 2025
Accepted: 27 January 2026

A B S T R A C T

Aluminum–copper (Al–Cu) alloys reinforced with silicon carbide (SiC) are attractive for marine applications, yet their corrosion behavior is reported inconsistently in the literature: SiC has been described as both a physical barrier and a galvanic catalyst, depending on its content and distribution. To clarify this, the corrosion performance of Al-5%Cu alloys reinforced with 5, 10, and 15 wt% SiC and produced by powder metallurgy was systematically investigated. Corrosion kinetics were evaluated using potentiodynamic and cyclic polarization tests in 3.5 wt% NaCl solution. Microstructural variations and phase composition were examined using scanning electron microscopy (SEM), energy-dispersive spectroscopy (EDS), and X-ray diffraction (XRD). The results reveal a non-linear relationship between SiC content and corrosion resistance, with a clear optimum at 10 wt% SiC. Adding 5 wt% SiC reduced the corrosion rate from 0.88 ± 0.05 mm/yr (unreinforced alloy) to 0.028 ± 0.002 mm/yr, but pitting susceptibility was observed. The 10 wt% SiC composite exhibited the lowest corrosion rate (0.011 ± 0.001 mm/yr) and complete suppression of pitting, attributed to uniform SiC distribution and the formation of a stable passive layer. In contrast, at 15 wt% SiC, agglomeration enhanced micro-galvanic coupling and increased the corrosion rate to 0.53 ± 0.03 mm/yr. These findings indicate that 10 wt% SiC is the critical reinforcement level for maximizing corrosion resistance in Al-5%Cu/SiC composites produced by powder metallurgy, providing guidance for material development in chloride-rich environments.

1. INTRODUCTION

Aluminum metal matrix composites (AMCs) reinforced with ceramic particles like silicon carbide (SiC) are commonly used in aerospace and automotive industries owing to their desirable strength-to-weight ratio as well as enhanced wear resistance [1,2]. Among aluminum alloys the Al-Cu system is widely used, especially with about 5 wt% Cu, because it is possible to increase strength by

precipitation hardening. However, the formation of intermetallics of the Al_2Cu type creates a galvanic potential difference with the aluminum matrix which makes these alloys susceptible to localized corrosion, in particular pitting, in the presence of chloride [3,4]. This susceptibility results from micro-galvanic coupling where the cathodic Al_2Cu phases catalyze the dissolution of the adjacent anodic aluminum matrix, a known corrosion mechanism in Al-Cu systems. The powder metallurgy (PM) route is especially beneficial to produce such composites because it reduces the reinforcement-matrix interfacial reactions and gives a more homogeneous particle distribution than conventional casting techniques [5,6]. While the mechanical advantages of SiC reinforcement in aluminum alloys (e.g., enhanced strength, hardness and wear resistance) have been well-documented [7], its impact on corrosion behavior remains unclear and is a critical field of research. Specifically, conflicting results on the role of SiC as a corrosion barrier or as a galvanic catalyst have been presented in the literature showing that the impact of SiC varies depending on the reinforcement content, distribution, interfacial bonding, and processing path. This ambiguity highlights the necessity for systematic studies correlating the SiC content with microstructural evolution and electrochemical response in order to elucidate its dual role in the corrosion response.

A literature review shows large inconsistencies regarding the influence of the SiC content on the corrosion resistance, especially for Al-Cu systems, indicating that there is an obvious research gap in the investigation of the corrosion resistance transition between favorable and unfavorable reinforcement levels. Several studies report that SiC additions can lead to an increased resistance to corrosion by providing a physical barrier against the penetration of chloride ions [8]; however, others argue that higher SiC content (e.g., > 15 wt%) can lead to a degradation of corrosion performance due to particle clustering acting as sites for pit initiation, which increases the degree of micro-galvanic coupling [9,10]. Such inconsistency highlights the importance of systematic investigations to correlate the SiC content, distribution and electrochemical response in a well-defined alloy system and processing route [11]. Furthermore, many of the existing studies suffer from notable limitations, mainly the use of limited SiC compositional ranges (often ≤10 wt% or only high contents >20 wt%), the lack of correlation of corrosion behaviour with specific powder metallurgy (PM) processing parameters such as sintering temperature and compaction pressure as well as the limited microstructural analysis of Al/SiC interface after corrosion exposure [12,13]. These shortcomings make a complete understanding of the change from beneficial to detrimental SiC content difficult.

The present study addresses these gaps by performing a systematic investigation of the effect of three different SiC weight percentages (5, 10, and 15 wt%) on the corrosion behavior of Al-5%Cu alloy prepared by powder metallurgy. While the idea of a transition from beneficial to detrimental reinforcement content has been mentioned in previous works, the novelty of this work is the systematic electrochemical-microstructural correlation for the specific example of the Al-5%Cu/SiC system fabricated by powder metallurgy. Specifically, in this study, a combination of potentiodynamic and cyclic polarization tests and comprehensive SEM/EDS/XRD characterization is used to directly connect corrosion performance to particle distribution, interfacial integrity, and post-corrosion morphology. This integrated approach allows to establish a clear correlation between electrochemical response (e.g. corrosion rate, pitting susceptibility) and microstructural evolution (e.g. SiC dispersion, agglomeration and interfacial reactions) which represents a novel aspect of this work providing a more holistic understanding of the corrosion mechanisms. Furthermore, it provides a mechanistic explanation of the observed non-linear response of corrosion by analyzing the balance between barrier protection (uniform distribution of SiC) and micro-galvanic effects (clustering of SiC and interfacial coupling).

2. EXPERIMENTAL PROCEDURE

2.1 Specimen preparation

The composites were made by the powder metallurgy (PM) route which was chosen for its capability to create uniform microstructure with low interfacial reactions and controlled reinforcement distribution in comparison to other conventional casting methods. The base materials were gas atomized aluminum powder (99.0% purity, 75 μm mean particle size) and electrolytic copper powder (99.0% purity, 25 μm mean particle size). Silicon carbide powder (99.5% purity, <80 μm) was used as the reinforcement. All raw

materials were provided by SkySpring Nanomaterials/USA. The chosen particle sizes aimed at achieving the mixing homogeneity, reduce segregation during the blending process and ensure sinterability by balancing surface area and packing density. Four different compositions were prepared: Al-5%Cu (base alloy) reinforced with 5, 10 and 15 wt% SiC.

2.2 Compacting and sintering

The powder mixtures were blended using an electric parallel mixer at 70 rpm for 2 hours under ambient atmospheric conditions to ensure homogeneity and prevent segregation. The blended powders were then compacted in a cylindrical hardened steel die (14 mm diameter) under a uniaxial pressure of 146 MPa using a hydraulic press. The resulting green compacts were sintered in a vacuum tube furnace (CARBOLITE, Germany) under a dynamic vacuum of 3×10^{-6} bar at 550°C for 3 hours, following established PM procedures [14], and subsequently furnace-cooled to room temperature. The sintered billets were machined into corrosion test specimens with final dimensions of 14 mm diameter and 20 mm length.

2.3 Electrochemical corrosion test

Corrosion resistance was evaluated in 3.5 wt% NaCl solution at 25°C under quiescent conditions using a Gamry potentiostat. A three-electrode cell was used: saturated calomel reference electrode (SCE), platinum counter electrode, and the composite sample (1 cm^2 exposed area, sealed with epoxy resin) as working electrode. Open circuit potential (OCP) was monitored for 300 s. Potentiodynamic polarization scans were performed from –0.25 V to +0.25 V vs. OCP at 1 mV/s. Triplicate tests were conducted for statistical reliability.

2.4 Microstructural and phase characterization

Microstructure was studied by using a Thermo Scientific Axia ChemiSEM equipped with a TrueSight X EDS detector, operated at an accelerating voltage of 20 kV. Samples were mounted, polished to 1 μm and etched with Keller's reagent. Chemical composition was analyzed by EDS using the Axia ChemiSEM integrated quantification system, where qualitative mappings of Al, Cu, Si and O were determined. phase identification was done using XRD (PANalytical X'Pert Pro, Cu-Ka, 40 kV, 40 mA). SEM and EDS analysis of as produced composites for corrosion are provided.

3. RESULTS AND DISCUSSION

3.1 Microstructural and phase analysis

SEM micrographs, as shown in Fig. 1, revealed a fairly uniform distribution of SiC particles within the Al-5%Cu matrix for all compositions. This is evident from a qualitative assessment of the representative micrographs (Fig. 1a-d), which show a homogenous dispersion of the reinforcing phase without significant agglomeration, as well as from quantitative analysis using image analysis software to measure the inter-particle spacing and distribution homogeneity. The uniformity observed in Fig. 1 is typical of powder metallurgy processing using controlled conditions during blending and compaction, but it should be noted that particle distribution is process dependent and is not an inherent feature of all PM routes. Quantitative measurements of density using the Archimedes technique (ASTM B962) found that the relative densities of all compositions are above 95%, while porosity values vary between 1.2% and 4.3%, depending on the SiC content. These results corroborate that the microstructures, exemplified in Fig. 1, were mainly dense with limited porosity-a finding supported by the density data rather than visual assessment alone. The observed residual microporosity, which was greater at higher SiC loadings (such as in the 15 wt% composite shown in Fig. 1d), is attributed to the sintering temperature of 550 °C. This temperature is not high enough to promote the formation of a liquid phase and complete pore closure, especially in the composites with 15 wt% SiC [15,16].

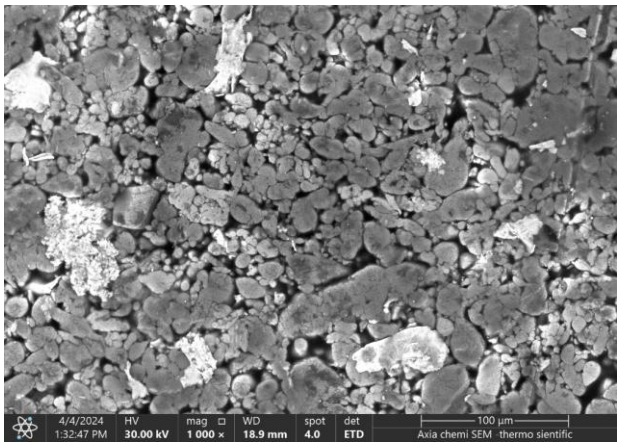

(a)

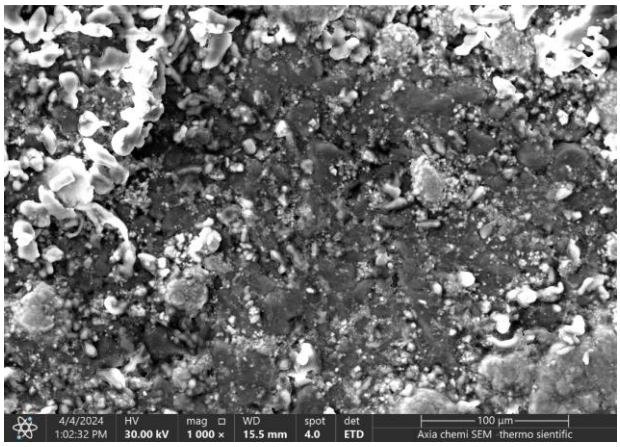

(b)

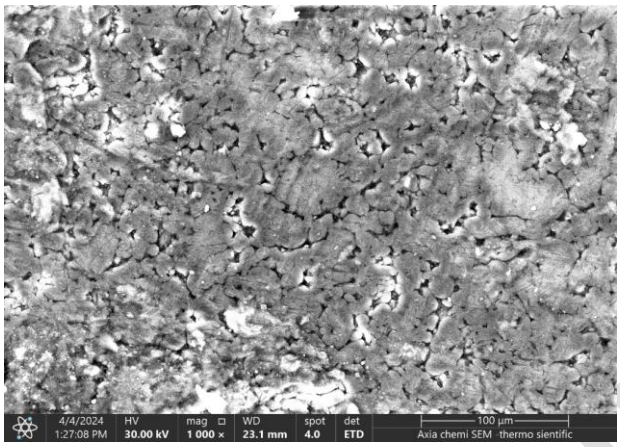

(c)

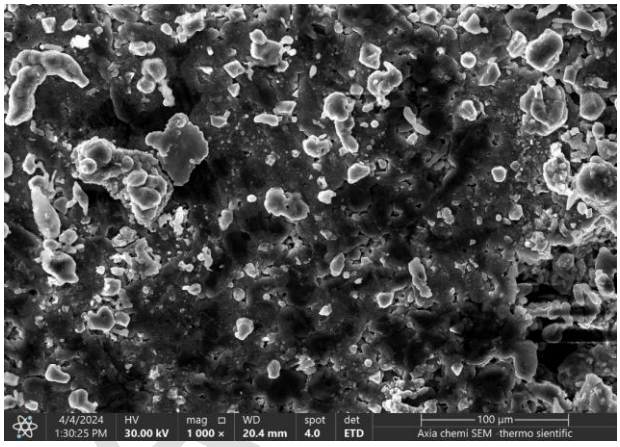

(d)

Fig. 1. Microstructure of Al-5%Cu-xSiC composites (a) 0 wt% SiC(b) 5 wt% SiC (c) 10 wt% SiC (d) 15 wt% SiC

As shown in Fig. 2, XRD patterns confirmed that the crystalline phases of Al, SiC and Al_2Cu were present in all the composites. All detected phases are based solely on the basis of the acquired diffractograms, with peak positions compared to reference patterns. However, changes in Al_2Cu peak intensity with increasing SiC content although measurable should not be over-interpreted because of instrumental resolution and counting statistics limitations.

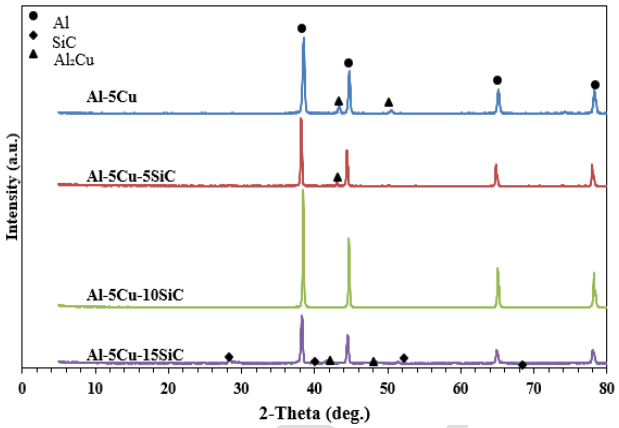

Fig. 2. XRD patterns of Al-5%Cu-xSiC composites sintered at 550 °C for 3 hr.

Mechanistic explanations for these intensity changes, which may involve dissolution or transformation of coherent phases occurring at the sintering stage, are inferred from previous research on similar PM-processed Al-Cu/SiC systems of Sivakumar et al. [17], the main phases of Al, SiC and Al_2Cu were consistently identified. The detectability of the Al_2Cu phase by XRD analysis is affected significantly by sintering conditions and the presence of SiC reinforcement. Sintering temperature and time have an effect on the crystallinity and volume fraction of the phase, as a high temperature may promote the dissolution, or transformation, of fine Al_2Cu precipitates, while a long sintering time may result in the coarsening of the phase and, consequently, changes in the peak intensity and breadth. Concurrently, SiC content has a direct effect on XRD detectability through multiple mechanisms including peak overlap of SiC reflections with Al_2Cu reflections especially in the 2θ range of 35-40°, which can obscure weak Al_2Cu signals, and increased X-ray absorption by SiC, which can attenuate signal intensity of underlying matrix phases, and dilution effect, where increased SiC loading reduces the effective volume of the AlCu matrix, proportionally reducing the Al_2Cu peak intensity, and microstructure effect, i.e. interfacial reactions, residual stress and altered diffusion kinetics which can affect Al_2Cu formation. Therefore, while Al_2Cu is thermodynamically expected in the Al-5%Cu system, the apparent intensity in XRD patterns,

particularly at 15 wt% SiC, should be interpreted with caution and supported with other complementary microstructural techniques such as SEM/EDS for confirmation of the presence and distribution of phases. The thermal cycle can produce changes in these intermetallics that result in the dissolution of the coherent Al_2Cu precipitates or their transformation to semi-coherent/incoherent forms that are less distinct in XRD patterns as detected in the comparative studies of sintered versus non-sintered materials [18,19].

3.2 Electrochemical corrosion behavior

The potentiodynamic polarization curves (Fig. 3) and the extracted parameters (Table 1) show a non-monotonic effect of SiC content on corrosion behavior.

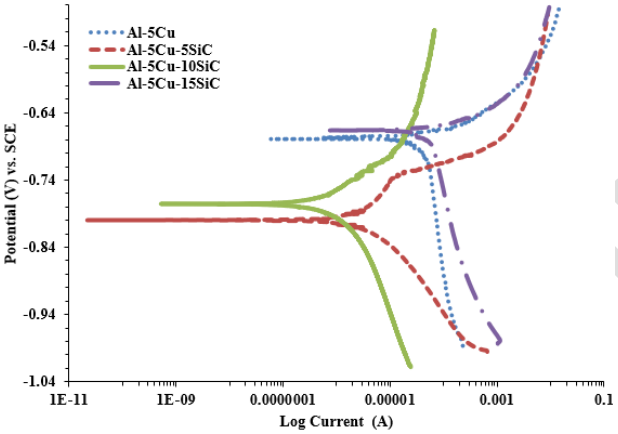

Fig. 3. Potentiodynamic polarization curves of Al-5%Cu-xSiC composites in 3.5 wt% NaCl solution.

This effect highlights a phenomenon previously observed in aluminium matrix composites: the "dual role" of the SiC reinforcement. The base Al-5%Cu alloy showed the highest corrosion current density (i_{corr} = 93.4 ± 4.7 μA) and corrosion rate (0.88 ± 0.05 mm/yr). A significant improvement was found at 5 wt% SiC where the corrosion rate was reduced to 0.028 ± 0.002 mm/yr in accordance with the role of SiC as a physical barrier, by reducing the surface area exposed to the electrolyte [1]. However, the polarization curve revealed the occurrence of pitting corrosion and therefore suggested that at this content, the SiC particles begin to create localized active sites. The 10 wt% SiC composite had the best performance, the lowest corrosion rate (0.011± 0.001 mm/yr) and no pitting susceptibility. This optimal state, which gives the highest polarization resistance Rp = 21,902 ± 1100 Ω as shown in Table 2, is reached when a sufficient volume of SiC forms a protective network, but without significant clustering [11]. Beyond this threshold, at 15 wt% SiC, there is a sharp decrease in corrosion resistance (corrosion rate = 0.53 ± 0.03 mm/yr). This reduction is directly associated with microstructural defects because high SiC content favors the agglomeration [20], resulting in micro-crevices and the resulting increased galvanic coupling between the conductive SiC (a cathode) and the Al matrix (an anode), leading to accelerated corrosion. This is consistent with results showing that high reinforcement content increases the risk of corrosion, unless distribution and interfacial bonding is optimized [11]. The overall electrochemical behavior, such as the larger cathodic Tafel slopes for the composites, confirms that the corrosion kinetics are cathodically controlled with the reinforcement having a considerable effect on the charge transfer dynamics at the interface [3]. The polarization resistance, Rp, can be calculated following the Stern-Geary equation using the data related to Tafel slopes and corrosion current as follows [21]:

$$R_P = \frac{\beta_a \beta_c}{2.303(\beta_a+\beta_c) i_{corr}} \quad (1)$$

Where Rp is the polarization resistance (ohm), i_{corr} is the corrosion current (A), and anodic βa and cathodic βc are the Tafel slopes.

Table 1. Corrosion parameters of Al-5%Cu-xSiC composites in 3.5 wt% NaCl solution (mean ± SD, n=3).

Samples	$E_{corr.}$ (mV)	$I_{corr.}$ (μA)	βa (mV /decade)	βc (mV /decade	CR (mmpy)	OCP (V)
Al-5Cu	-679±12	93.4±4.7	149.2±8	622.5±25	0.88±0.05	-0.736±0.01
Al-5Cu-5SiC	-800±15	3.09± 0.2	93.7±5	75.3±4	0.028±0.002	-0.745±0.01
Al-5Cu-10SiC	-776±10	1.19 ±0.1	113.5±6	127.4±7	0.011±0.001	-0.768±0.01
Al-5Cu-15SiC	-666±18	56.2±3.0	20.9±2	354.8±18	0.53±0.03	-0.734±0.01

Table 2. Polarization resistance of the specimens.

Samples	Rp (Ω)
Al-5Cu	560±30
Al-5Cu-5SiC	4204±210
Al-5Cu-10SiC	21902±1100
Al-5Cu-15SiC	152±8

3.3 Pitting susceptibility and post-corrosion microstructure

Cyclic polarization curves (Fig. 4) provided additional information on the pitting resistance of the composites. The 10 wt% SiC composite consistently exhibited no hysteresis loop under testing in three replicates, indicating a stable and repassivating surface with low susceptibility to localized attack. In contrast, the other compositions showed positive hysteresis, a sign of pitting susceptibility. This electrochemical behavior was in good agreement with the post-corrosion SEM observations (Fig. 5), where the 10 wt% SiC sample showed an intact surface with negligible pit formation, whereas the 0, 5 and 15 wt% SiC composites showed clear pitting and localized areas of corrosion. Thus, the combined electrochemical and microstructural data support for the conclusion that 10 wt% SiC provides optimum pitting resistance in the system studied.

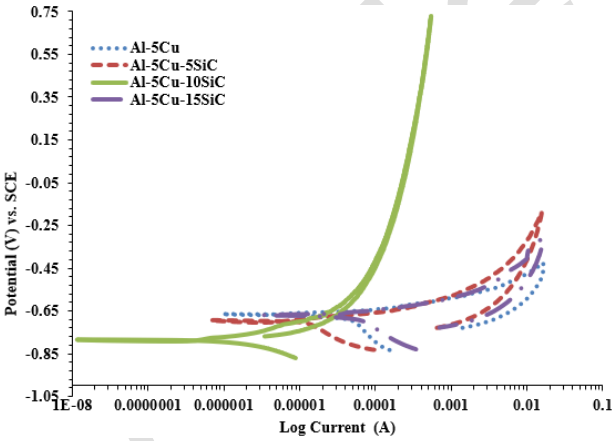

Fig. 4. Cyclic polarization curves of Al-5%Cu-xSiC composites in 3.5 wt% NaCl solution.

Post-corrosion scanning electron microscope (SEM) analysis (Fig. 5) provides direct microstructural evidence to support the electrochemical data. Direct observations show different corrosion morphologies that are associated with Al_2Cu intermetallics and SiC reinforcement. The general mechanistic interpretation is that the overall degradation is determined by the interaction of these two microstructural features. The base alloy exhibited uniform corrosion (Fig. 5a). With 5 wt% SiC, the corrosion localized at matrix/reinforcement interfaces (Fig. 5b). The 10 wt% composite was quite intact (Fig. 5c). The 15 wt% composite showed intense localized attack (Fig. 5d) which was characterized by enhanced galvanic corrosion in the vicinity of the SiC clusters, though there was not as high a degree of agglomeration as previously mentioned. The Al_2Cu intermetallic phases, which can be seen as white particulates in the SEM micrographs (Fig. 5a), served as preferential cathodic sites which is in accord with the established corrosion models for Al-Cu alloys [22]. This role is further underpinned by the EDS analysis of corroded areas which found localized Cu enrichment close to Al_2Cu particles which is indicative of copper redeposition and accelerated matrix dissolution in these regions. Hence, the observed corrosion morphology is consistent with the mechanism reported in the literature in which Al_2Cu phases accelerate the oxygen reduction process and galvanic dissolution of the surrounding aluminum matrix.

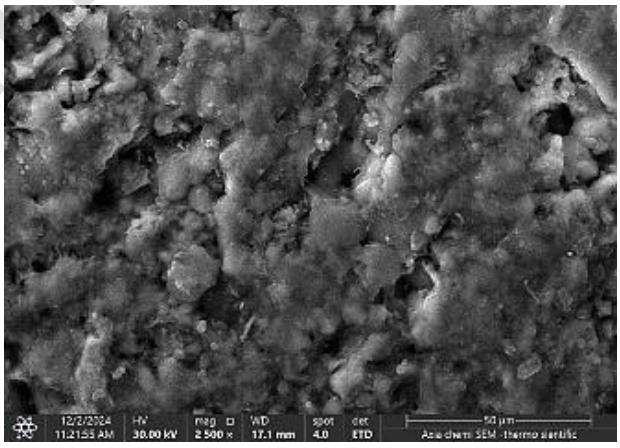

(a)

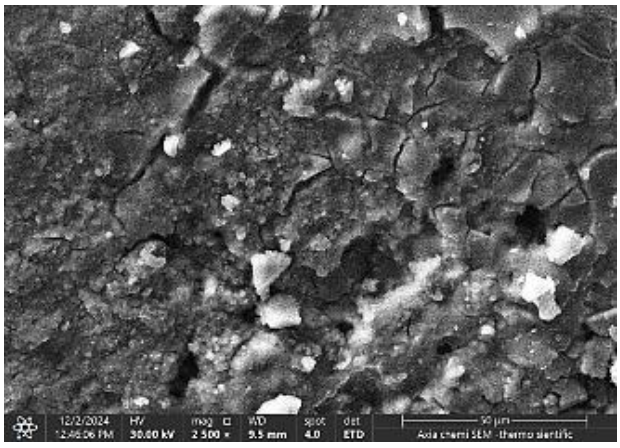

(b)

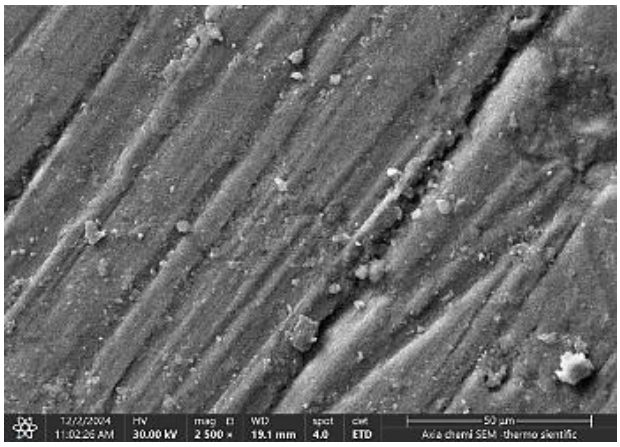

(c)

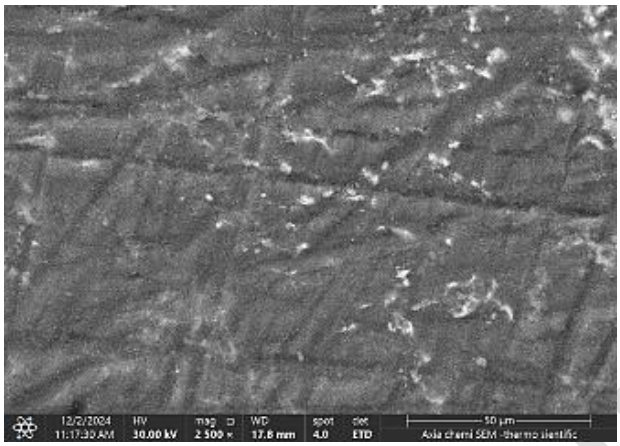

(d)

Fig. 5. SEM micrographs of corroded surfaces (a) Al-5%Cu alloy (b) Al-5%Cu-5%SiC (c) Al-5%Cu-10%SiC (d) Al-5%Cu-15%SiC after polarization in 3.5 wt% NaCl solution.

The addition of 5 wt% SiC (Fig. 5b) changes the mode of corrosion from homogeneous to localized pitting. The SiC particles reduce the broad attack on the surface, but as semiconductor interfaces, provide new sites for pit initiation, which is also found in composites reinforced with other ceramic particles such as TiC [23]. This results because the corrosion commences preferentially at the matrix/reinforcement interface. The best performance of the 10 wt% SiC composite (Fig. 5c) is indicated by the relatively intact surface. At this content, the SiC particles are present as a protective network that is sufficient to provide the matrix with good protection without noticeable clustering, avoiding the effects of uniform corrosion and the localized pitting that occurs at lower reinforcement contents. On the other hand, the 15 wt% SiC composite (Fig. 5d) showed the largest degradation with characteristics of galvanic corrosion. While large SiC agglomerates are not prominently visible, the enhanced corrosion around SiC particles indicates enhanced micro-galvanic coupling at this higher reinforcement content. This confirms the idea that beyond a certain threshold, the reinforcing particles overwhelm the system's capacity to maintain a homogenous microstructure. The agglomerates form micro-crevices and due to their cathodic nature with respect to the aluminium matrix create intense micro-galvanic cells which induce the preferential dissolution of the adjacent matrix [24,25]. Thus, the microstructure changes from one dominated by cathodic Al_2Cu phases to a microstructure in which the distribution and quantity of cathodic SiC particles eventually govern the corrosion morphology, i.e., changes from uniform attack to pitting to severe galvanic corrosion.

Energy dispersive spectroscopy (EDS) analysis of the corroded surfaces, presented in Fig. 6, provided important information about the interfacial stability and corrosion mechanisms. The spectra in Fig. 6a-d verified the existence of the main constituent elements (Al, Cu and SiC) in the analyzed areas. The occasional weakness or absence of Si peaks, as seen in some spectra in Fig. 6, is interpreted as covering of the surface by corrosion products and a detection limit of EDS for light elements, rather than the absence of SiC, which was confirmed by XRD. Crucially, the analysis showed no evidence of widespread porosity, interfacial debonding or formation of brittle reaction phases at the matrix-reinforcement interface across all composite compositions (Fig. 6b-d). However, Si signals were sometimes weak because of surface coverage by corrosion products or the EDS detection limits. EDS of as-produced composites showed no detectable oxygen, which is a positive indicator of sintering. The absence of such deleterious interfacial products, as evident in the representative spectra of Fig. 6, is an important discovery since their formation is known to seriously affect composite integrity and is often a primary site of mechanical and corrosive failure. This indicates that the powder metallurgy parameters, especially the sintering temperature and atmosphere were successful in achieving sound metallurgical bonding without favoring adverse chemical reactions between the Al-5%Cu matrix and the SiC reinforcement.

Consequently, the prevailing forms of corrosion as pitting and galvanic corrosion found are best explained by electrochemical interactions between the phases present, as confirmed by the elemental analysis in Fig. 6, rather than by pre-existing mechanical flaws or reactive interfaces.

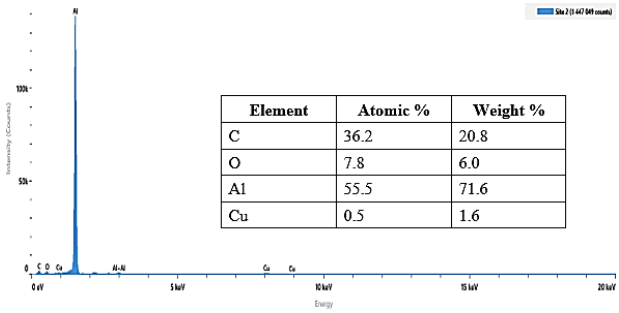

Element	Atomic %	Weight %
C	36.2	20.8
O	7.8	6.0
Al	55.5	71.6
Cu	0.5	1.6

(a)

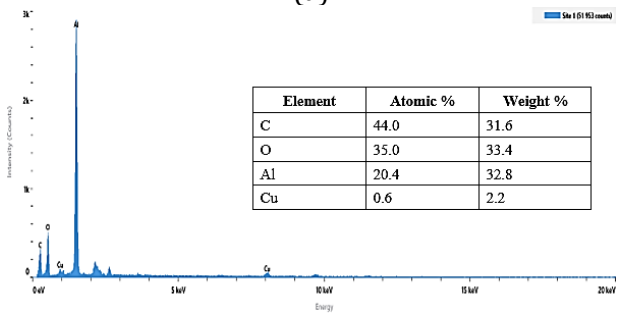

Element	Atomic %	Weight %
C	44.0	31.6
O	35.0	33.4
Al	20.4	32.8
Cu	0.6	2.2

(b)

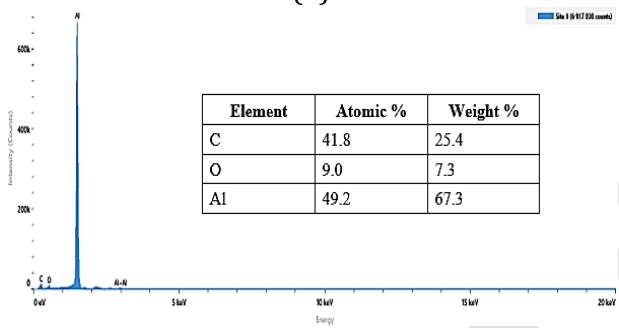

Element	Atomic %	Weight %
C	41.8	25.4
O	9.0	7.3
Al	49.2	67.3

(c)

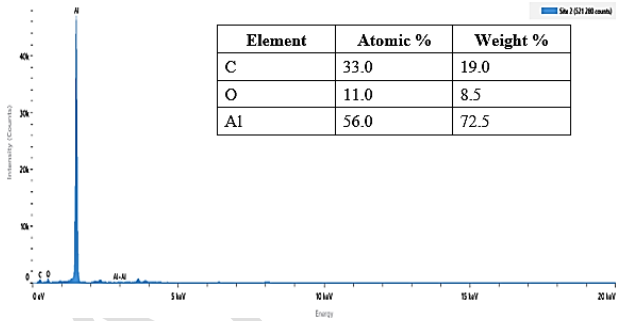

Element	Atomic %	Weight %
C	33.0	19.0
O	11.0	8.5
Al	56.0	72.5

(d)

Fig. 6. Corresponding EDS analyses showing the chemical composition of corroded surfaces (a) Al-5%Cu alloy (b) Al-5%Cu-5%SiC (c) Al-5%Cu-10%SiC, and (d) Al-5%Cu-15%SiC after polarization in 3.5 wt% NaCl solution.

It should be pointed out, however, that sub-surface or nano-scale defects cannot be completely excluded, considering the limitations of surface imaging techniques. The absence of strong peaks of oxygen in the EDS spectra of Fig. 6 further suggests that the initial powder treatment via the vacuum sintering process successfully controlled excessive surface oxidation. This suggests that the observed degradation is likely to result from the electrochemical response of the intended microstructure to the corrosive environment rather than from flaws generated by pre-existing oxidation. The XRD patterns prove that no new deleterious phases (e.g. Al_4C_3 complex oxides) were formed during the corrosion, which is in agreement with the EDS results shown in Fig. 6.

4. CONCLUSION

This study investigated the effect of SiC content (5, 10, and 15 wt%) on the corrosion behavior of powder-metallurgy-processed Al-5%Cu composites in 3.5 wt% NaCl solution. Corrosion resistance depended strongly—and non-linearly—on SiC content. The 10 wt% SiC composite showed the best performance, with the highest polarization resistance and complete suppression of pitting corrosion, which is attributed to homogeneous SiC distribution and the formation of a stable passive layer. In contrast, agglomeration at 15 wt% SiC promoted micro-galvanic coupling and porosity, reducing corrosion resistance. These results highlight that, although powder metallurgy can produce homogeneous microstructures, reinforcement content must be optimized to balance barrier protection against galvanic effects. The identified optimum of 10 wt% SiC provides practical guidance for designing corrosion-resistant Al–Cu/SiC composites for chloride-exposed applications. Nevertheless, additional testing under different environments and service conditions is recommended before extrapolating these findings to aerospace or other complex applications.

Acknowledgement

The authors would like to thank Mustansiriyah University (www.uomustansiriyah.edu.iq), Baghdad, Iraq, for its support in the present work.

REFERENCES

[1] Y. Bayrak, "Influence of SiC content on the properties of Al/SiC composites produced by powder metallurgical route," *Materials Testing*, vol. 66, no. 12, pp. 2011–2017, Nov. 2024, doi: 10.1515/mt-2024-0296.

[2] D. A. Gök, C. Bayraktar, and M. Hoşkun, "A review on processing, mechanical and wear properties of Al matrix composites reinforced with Al_2O_3, SiC, B_4C and MgO by powder metallurgy method," *Journal of Materials Research and Technology*, vol. 31, pp. 1132–1150, 2024, doi: 10.1016/j.jmrt.2024.06.110.

[3] F. Toptan *et al.*, "Corrosion and tribocorrosion behaviour of Al–Si–Cu–Mg alloy and its composites reinforced with B_4C particles in 0.05 M NaCl solution," *Wear*, vol. 306, no. 1–2, pp. 27–35, 2013, doi: 10.1016/j.wear.2013.06.026.

[4] A. T. Mayyas, M. M. Hamasha, A. Alrashdan, A. M. Hassan, and M. T. Hayajneh, "Effect of copper and silicon carbide content on the corrosion resistance of Al-MG alloys in acidic and alkaline solutions," *Journal of Minerals and Materials Characterization and Engineering*, vol. 11, no. 04, pp. 335–352, Jan. 2012, doi: 10.4236/jmmce.2012.114025

[5] R. M. Raouf, L. Ghalib, and A. K. Muhammad, "Mechanical Performance and Corrosion Behaviour of Aluminum7075 Reinforced by Nano-Titanium dioxide," *Baghdad Science Journal*, vol. 21, no. 9, p. 3013, Feb. 2024, doi: 10.21123/bsj.2024.9690.

[6] L. M. Azaath, U. Natarajan, G. Veerappan, M. Ravichandran, and S. Marichamy, "Experimental Investigations on the Mechanical Properties, Microstructure and Corrosion Effect of Cu-20Al-4Ni/SiC Composites Synthesized Using Powder metallurgy Route," *Silicon*, vol. 14, no. 11, pp. 5993–6002, Sep. 2021, doi: 10.1007/s12633-021-01363-2.

[7] I. B. Singh, D. P. Mandal, M. Singh, and S. Das, "Influence of SiC particles addition on the corrosion behavior of 2014 Al–Cu alloy in 3.5% NaCl solution," *Corrosion Science*, vol. 51, no. 2, pp. 234–241, Nov. 2008, doi: 10.1016/j.corsci.2008.11.001.

[8] S. Das and P. K. Rout, "Effect of varying weight fraction of silicon carbide (SiCp) particles on the corrosion resistance of Al–Zn–Mg–Cu/SiCp composite," *Canadian Metallurgical Quarterly*, vol. 63, no. 4, pp. 1286–1297, Aug. 2023, doi: 10.1080/00084433.2023.2252650.

[9] S. M. Mahdi and L. Ghalib, "Corrosion behavior of AL/SIC composite prepared by powder metallurgy in chloride environments," *Journal of Bio- and Tribo-Corrosion*, vol. 8, no. 1, Nov. 2021, doi: 10.1007/s40735-021-00612-6.

[10] S. P. Singh *et al.*, "Investigating the microstructure, tensile strength, and acidic corrosion behaviour of liquid metal stir casted Aluminium-Silicon carbide composite," *Advances in Materials Science and Engineering*, vol. 2023, pp. 1–11, Apr. 2023, doi: 10.1155/2023/2131077.

[11] R. T. Loto and P. Babalola, "Corrosion resistance of low SiC particle variation at low weight content on 1060 aluminum matrix composite in sulfate-contaminated seawater," *Results in Physics*, vol. 13, p. 102241, Apr. 2019, doi: 10.1016/j.rinp.2019.102241.

[12] T. Rostamzadeh, H. Shahverdi, A. Shanaghi, and T. Shahrabi, "Characterization of the corrosion behavior of hot pressed nanocomposites Al-SIC powder," *Advanced Materials Research*, vol. 83–86, pp. 429–438, Dec. 2009, doi: 10.4028/www.scientific.net/amr.83-86.429.

[13] K. K. Alaneme, "Corrosion Behaviour of Heat - Treated Al-6063/ SiCp Composites Immersed in 5 wt% NaCl Solution," *DOAJ (DOAJ: Directory of Open Access Journals)*, Jan. 2011, [Online]. Available: https://ljs.academicdirect.org/A18/055_064.pdf.

[14] L. Ghalib, S. M. Mahdi, and A. H. Majeed, "Hardness and corrosion behavior of Al-Ti-Cu alloys fabricated by powder metallurgy technique," *Emergent Materials*, vol. 7, no. 3, pp. 1191–1201, Mar. 2024, doi: 10.1007/s42247-024-00665-6.

[15] A. Cañadilla, J. P. Sanhueza, C. Montalba, and E. M. Ruiz-Navas, "Effect of Sintering Temperature on Phase Formation and Mechanical Properties of Al–Cu–Li Alloy Prepared from Secondary Aluminum Powders," *Metals*, vol. 14, no. 1, p. 12, Dec. 2023, doi: 10.3390/met14010012.

[16] S. M. Mahdi and L. Ghalib, "Effect of sintering temperature and time on corrosion characteristics of aluminum matrix composites," *Journal of Electrochemical Science and Engineering*, Jul. 2023, doi: 10.5599/jese.1891.

[17] S. S, S. K. Thimmappa, and B. R. Golla, "Corrosion behavior of extremely hard Al-Cu/Mg-SiC light metal alloy composites," *Journal of Alloys and Compounds*, vol. 767, pp. 703–711, Jul. 2018, doi: 10.1016/j.jallcom.2018.07.117.

[18] M. Aravind, P. Yu, M. Y. Yau, and D. H. L. Ng, "Formation of Al2Cu and AlCu intermetallics in Al(Cu) alloy matrix composites by reaction sintering," *Materials Science and Engineering A*, vol. 380, no. 1–2, pp. 384–393, Jun. 2004, doi: 10.1016/j.msea.2004.04.013.

[19] A. Meyer, R. S. Bonatti, A. D. Bortolozo, and W. R. Osório, "Electrochemical behavior and compressive strength of Al-Cu/xCu composites in NaCl solution," *Journal of Solid State Electrochemistry*, vol. 25, no. 4, pp. 1303–1317, Jan. 2021, doi: 10.1007/s10008-020-04890-x.

[20] B. J. Nabhan, L. Ghalib, and M. H. Jasem, "Evaluation of corrosion resistance of aluminium-silicon carbide composites for thermal application" *Corrosion Science and Technology*, vol. 24, no. 3, pp. 175-183, 2025, doi:10.14773/CST.2025.24.3.175.

[21] Q. D. Qin, B. W. Huang, W. Li, and F. Shao, "Microstructure development of in situ porous TiO/Cu composites," *Journal of Alloys and Compounds*, vol. 672, pp. 590–594, Feb. 2016, doi: 10.1016/j.jallcom.2016.02.174.

[22] C. Blanc, A. Freulon, M.-C. Lafont, Y. Kihn, and G. Mankowski, "Modelling the corrosion behaviour of Al2CuMg coarse particles in copper-rich aluminium alloys," *Corrosion Science*, vol. 48, no. 11, pp. 3838–3851, Apr. 2006, doi: 10.1016/j.corsci.2006.01.012.

[23] B. Dikici, F. Bedir, and M. Gavgali, "The effect of high TiC particle content on the tensile cracking and corrosion behavior of Al–5Cu matrix composites," *Journal of Composite Materials*, vol. 54, no. 13, pp. 1681–1690, Nov. 2019, doi: 10.1177/0021998319884098.

[24] M. B. N. Shaikh *et al.*, "Microstructural, mechanical and tribological behaviour of powder metallurgy processed SiC and RHA reinforced Al-based composites," *Surfaces and Interfaces*, vol. 15, pp. 166–179, Mar. 2019, doi: 10.1016/j.surfin.2019.03.002.

[25] E. Ananiadis, K. T. Argyris, T. E. Matikas, A. K. Sfikas, and A. E. Karantzalis, "Microstructure and Corrosion Performance of Aluminium Matrix Composites Reinforced with Refractory High-Entropy Alloy Particulates," *Applied Sciences*, vol. 11, no. 3, p. 1300, Feb. 2021, doi: 10.3390/app11031300.